

The Long-Life Li–S Batteries Based on Enabling Immobilization and Catalytic Conversion of Polysulfides.

Yupeng Zhang^a, Rong Gu^a, Shuai Zheng^a, KeXuan Liao^a, Penghui Shi^{a,b,c},

Jinchen Fan^{a,b*}, QunJie Xu^{a,b*}, YuLin Min^{a,b*}

^aShanghai Key Laboratory of Materials Protection and Advanced Materials

in Electric Power, Shanghai University of Electric Power, Shanghai 200090, P.R. China

^bShanghai Institute of Pollution Control and Ecological Security,
Shanghai 200092, P.R. China

^cHenan Province Key Laboratory of Water Pollution Control and Rehabilitation Technology

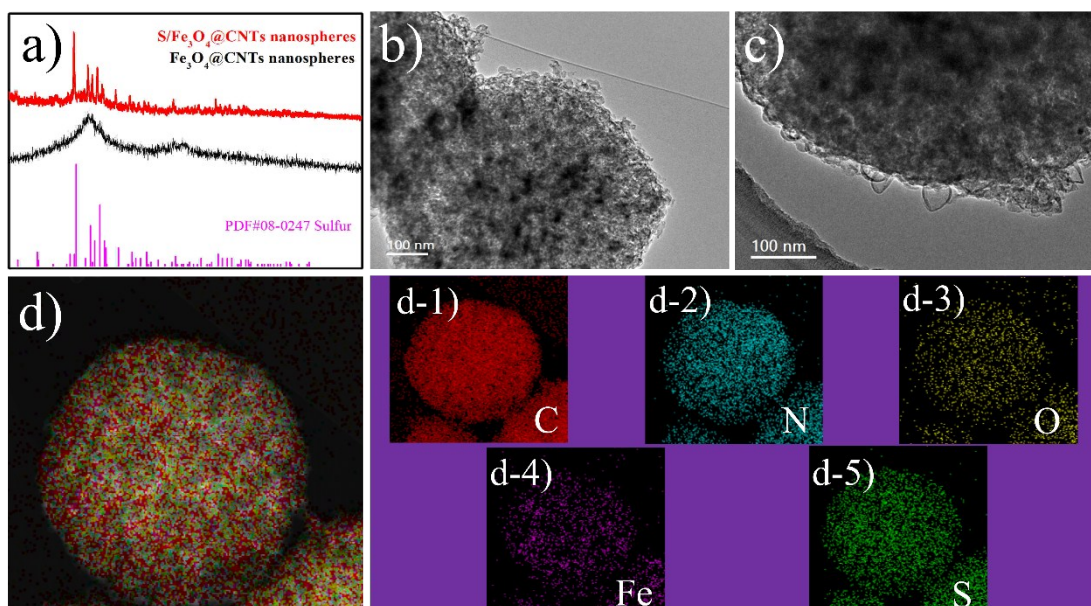


Fig. S1. Morphology and composition characterizations of S/Fe₃O₄@CNTs nanospheres composites: a) XRD pattern, (b,c) TEM images and (d) corresponding elemental mappings of the S/Fe₃O₄@CNTs nanospheres composites.

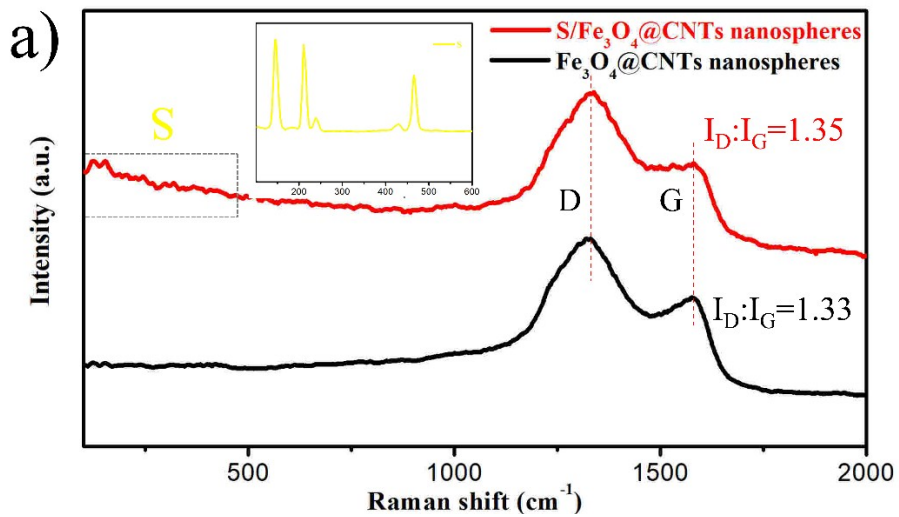


Fig. S2. a) Raman spectra of $\text{Fe}_3\text{O}_4@\text{CNTs}$ nanospheres and $\text{S}/\text{Fe}_3\text{O}_4@\text{CNTs}$ nanospheres

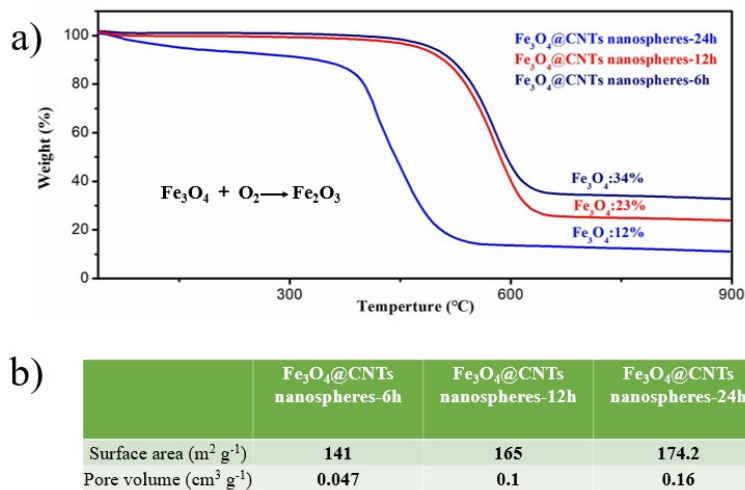


Fig. S3. a) TGA curve of $\text{Fe}_3\text{O}_4@\text{CNTs}$ nanospheres in air; b) surface area and pore volume of the $\text{Fe}_3\text{O}_4@\text{CNTs}$ nanospheres-6 h, $\text{Fe}_3\text{O}_4@\text{CNTs}$ nanospheres-12 h and $\text{Fe}_3\text{O}_4@\text{CNTs}$ nanospheres-24 h

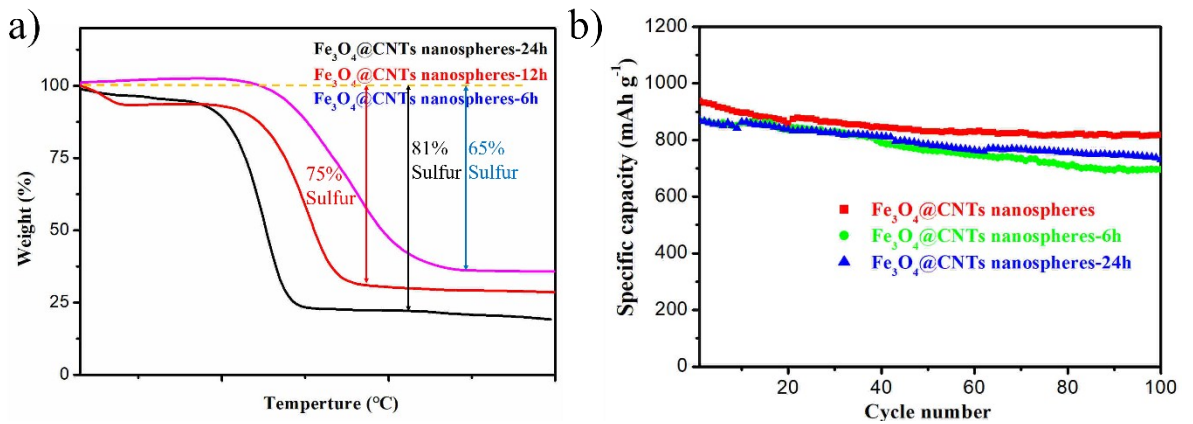


Fig. S4. a) TG curves of S/ Fe_3O_4 @CNTs nanospheres-6 h, S/ Fe_3O_4 @CNTs nanospheres-12 h, and S/ Fe_3O_4 @CNTs nanospheres-24 h b) Corresponding cyclic performance at 1C over 100 cycles with 2.1 mg cm⁻² sulfur loading

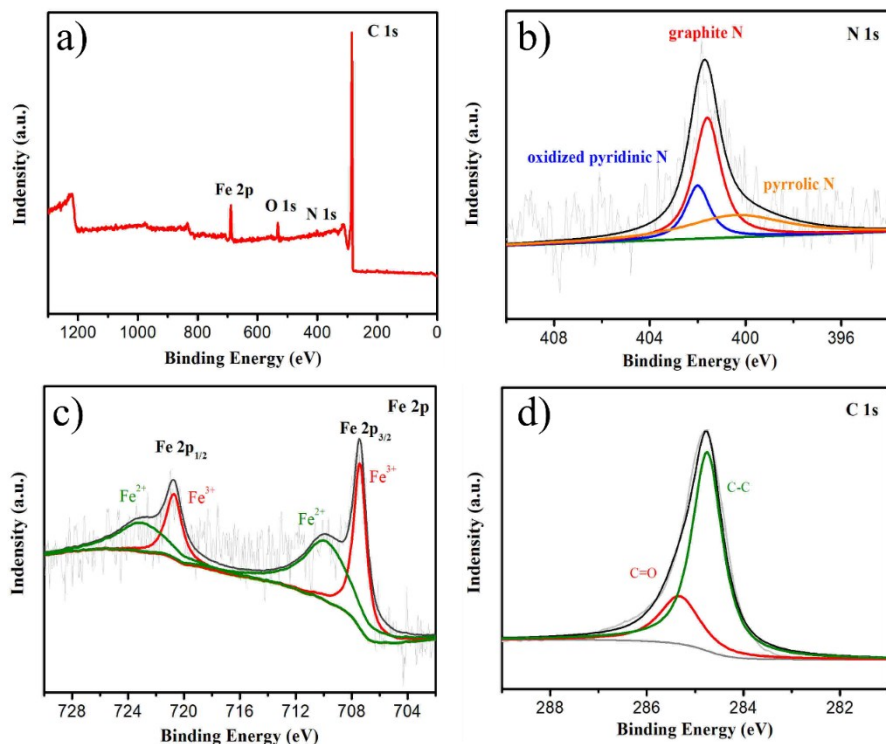


Fig. S5. (a) XPS spectra of Fe_3O_4 @CNTs nanospheres; and (b-d) the high resolution XPS spectra of N 1s, C 1s, and Fe 2p

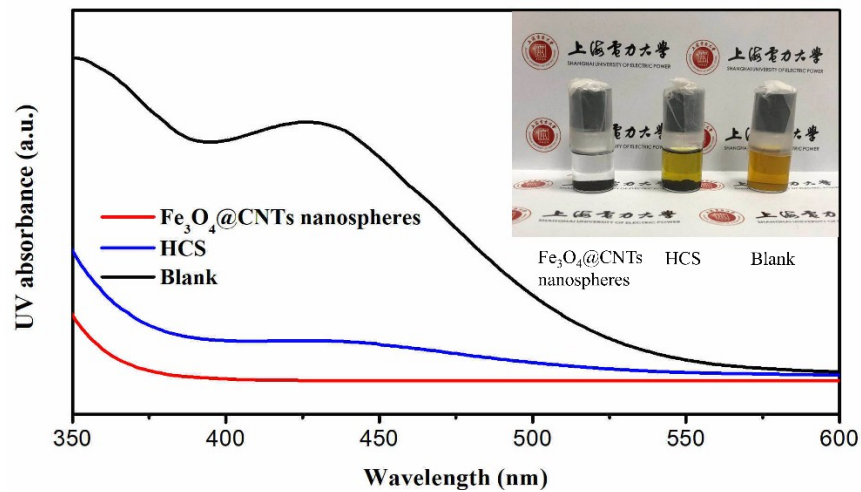


Fig. S6. UV-vis absorption spectra of Li_2S_4 solution mixed with $\text{Fe}_3\text{O}_4@\text{CNTs}$ nanospheres and HCS after standing for half an hour

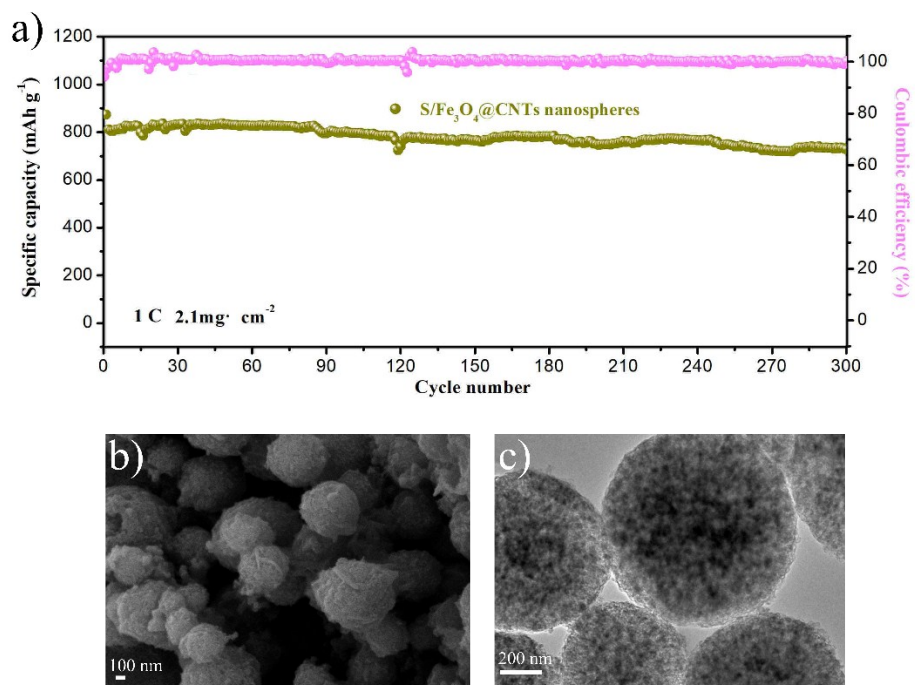


Fig. S7. a) Cycling test of the $\text{S}/\text{Fe}_3\text{O}_4@\text{CNTs}$ nanospheres at 2 C over 300 cycles
b) SEM image c) TEM image of $\text{S}/\text{Fe}_3\text{O}_4@\text{CNTs}$ nanospheres after the cycle.

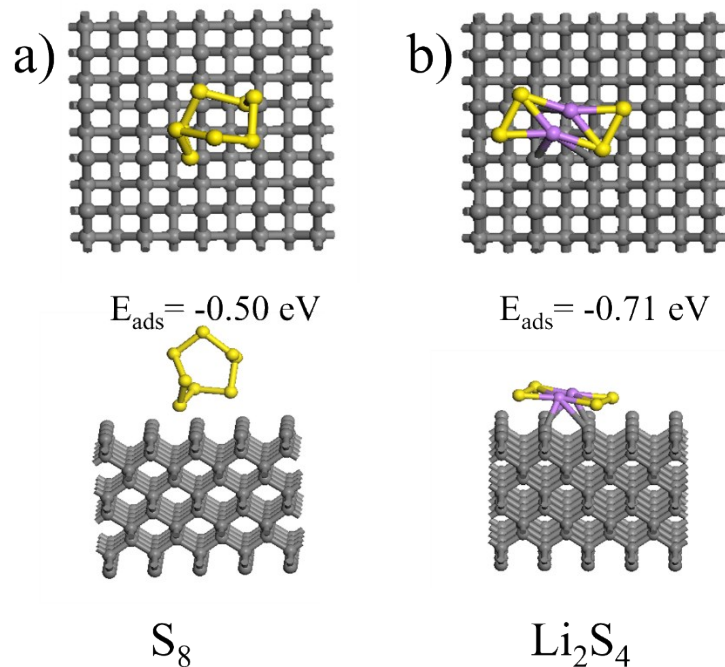


Fig. S8. binding geometric configurations and binding energies of S_8 and Li_2S_4 species with graphene

Table S1. Li-S batteries properties of various carbon-based cathode materials

Materials	Sulfur content (wt%)	Sulfur loading/mg cm ⁻²	Cycling performance		Rate of capacity decay per cycle	Ref.
			Cycle No.	Capacity/mAh g ⁻¹		
$\text{Fe}_3\text{O}_4@\text{CNTs}$ nanospheres	75wt%	2.1	1800	538.5 (1C)	0.023%	This Work
p-CNT@Void@MnO ₂	65wt%		100	526.1 (1C)	0.12%	1
Crumpled N-Ti ₃ C ₂ T _x	73wt%	1.5	200	950 (0.2C)	0.08%	2
$\text{Ba}_{0.5}\text{Sr}_{0.5}\text{Co}_{0.8}\text{Fe}_{0.2}\text{O}_{3-\delta}$ perovskite nanoparticles	63wt%	1.1	400	632 (0.5C)	0.05%	3
W ₂ C NPs-CNFs			400	605 (1C)	0.06%	4

P@E-CNTs	72wt%	2	200	735 (0.5C)	0.13%	5
GN-CNT	75wt%	1.6	500	363.5(1C)	0.09%	6
PPy-MnO₂	70wt%	2	500	550 (1C)	0.07%	7

References

1. Q. Liu, J. Zhang, S. A. He, R. Zou, C. Xu, Z. Cui, X. Huang, G. Guan, W. Zhang, K. Xu and J. Hu, *Small*, 2018, **14**, e1703816.
2. W. Bao, L. Liu, C. Wang, S. Choi, D. Wang and G. Wang, *Advanced Energy Materials*, 2018, **8**, 1702485.
3. L. Kong, X. Chen, B. Q. Li, H. J. Peng, J. Q. Huang, J. Xie and Q. Zhang, *Advanced materials*, 2018, **30**.
4. F. Zhou, Z. Li, X. Luo, T. Wu, B. Jiang, L. L. Lu, H. B. Yao, M. Antonietti and S. H. Yu, *Nano letters*, 2018, **18**, 1035–1043.
5. M. Yan, H. Chen, Y. Yu, H. Zhao, C.-F. Li, Z.-Y. Hu, P. Wu, L. Chen, H. Wang, D. Peng, H. Gao, T. Hasan, Y. Li and B.-L. Su, *Advanced Energy Materials*, 2018, **8**, 1801066.
6. Z. Zhang, L.-L. Kong, S. Liu, G.-R. Li and X.-P. Gao, *Advanced Energy Materials*, 2017, **7**, 1602543.
7. J. Zhang, Y. Shi, Y. Ding, W. Zhang and G. Yu, *Nano letters*, 2016, **16**, 7276–7281.